Scientific Research Publishing

Open Journal of Civil Engineering, 2023, 13, 555-571
https://www.scirp.org/journal/ojce
ISSN Online: 2164-3172
ISSN Print: 2164-3164

Comprehensive Analysis Method of Slope Stability Based on the Limit Equilibrium and Finite Element Methods and Its Application

Yajun Wang[1], Yifeng Li[1*], Jinzhou Chen[2]

[1]School of Civil Engineering and Architecture, Wuhan Institute of Technology, Wuhan, China
[2]Guangdong Geological Engineering Company, Guangzhou, China
Email: yajun11616@163.com, *749835857@qq.com, zsb@wit.edu.cn

How to cite this paper: Wang, Y.J., Li, Y.F. and Chen, J.Z. (2023) Comprehensive Analysis Method of Slope Stability Based on the Limit Equilibrium and Finite Element Methods and Its Application. *Open Journal of Civil Engineering*, **13**, 555-571.
https://doi.org/10.4236/ojce.2023.134040

Received: September 13, 2023
Accepted: October 31, 2023
Published: November 3, 2023

Abstract

To study the safety and stability of large slopes, taking the right side slope of the Yuxi'an tunnel of the Yuchu Expressway Bridge in Yunnan Province as an example, limit equilibrium and finite element analysis were applied to engineering examples to calculate the stability coefficient of the slope before and after excavation in the natural state. After comparative analysis, it was concluded that the former had a clear mechanical model and concept, which could quickly provide stability results; the latter could accurately determine the sliding surface of the slope and simulate the stress state changes of the rock and soil mass. The stability coefficients calculated by the two methods were within the stable range, but their values were different. On this basis, combined with the calculation principles, advantages and disadvantages of the two methods, a comprehensive analysis method of slope stability based on the limit equilibrium and finite element methods was proposed, and the rationality of the stability coefficient calculated by this method was judged for a slope case.

Keywords

Slope Body Excavation, Mechanical Model, Sliding Surface, Coefficient of Stability, Calculation Principle, Comprehensive Analysis Method

1. Introduction

In recent years, with the fundamental deployment of the national transportation network and the active promotion of the Western Development Strategy in China, infrastructure construction in the western regions has been growing. An

increasing number of large and medium-sized bridges and highways are being constructed. In the construction process, it is inevitable that roadbed excavation and earth filling activities will take place. These activities often trigger slope instability and damage issues, which have become a growing concern affecting the safety of people's lives in China [1] [2] [3] [4]. Due to environmental and construction conditions, slope engineering in complex environments is not uncommon, and the degree of hazard and the complexity of remediation processes associated with such slopes are considerable. Without a clear understanding and timely prevention and treatment, slope failures such as landslides and collapses can occur, jeopardizing people's lives and property.

The stability of slopes has long been a complex geotechnical issue in the field of engineering and has received extensive research and attention. Currently, analyses and research on slope stability are still theoretically lagging behind practice, and the accuracy of evaluations depends on the specific circumstances [5] [6] [7] [8] [9]. To address slope instability and failure problems, numerous slope evaluation methods have been proposed. At present, the most widely used methods can be roughly classified into two categories: one is the limit equilibrium method based on the Mohr-Coulomb criterion, and the other is the finite element method based on numerical calculations [10]. The former, with its simple mechanical models and vector operations, is applicable to most engineering problems, but its accuracy decreases for slopes with complex environmental conditions. With the advancement and development of computer technology, the finite element method, which uses numerical models for analysis, is becoming more common. However, the reliability of the results obtained by this method still needs to be verified in more engineering practices [11] [12] [13].

To develop a clearer understanding of these two methods and determine their applicability to different engineering problems, a comparative study of their results is essential. Therefore, in this study, we focus on the right-side slope of the Yuxi Tunnel of the Yuchu Expressway Bridge in Yunnan Province, China. We employ the limit equilibrium method and Midas GTS NX 2019 finite element analysis software to calculate its stability. By comparing the results obtained by these two methods, we assess their accuracy and differences. Furthermore, we propose a comprehensive slope stability analysis method based on both approaches to calculate stability coefficients that better reflect the practical conditions.

2. Slope Stability Analysis Methods

2.1. Limit Equilibrium Method for Slope Stability Analysis

In essence, the limit equilibrium method involves conducting a force analysis of an object under extreme conditions. This method is guided by the Mohr-Coulomb law and typically assumes a stability factor denoted as "K" for the research subject. It approximates the slope as a rigid body and, based on the static equilibrium relationship between the slope and sliding blocks on it, analyzes the re-

sisting forces and driving forces on the sliding blocks along the sliding surface. When a specific sliding surface reaches a state of limit equilibrium, the ratio of resisting forces to driving forces represents the safety factor. This approach investigates the stress state at the point of failure without considering the influence of the slope's inherent conditions [14].

In this study, we employ the coefficient of transmission method within the limit equilibrium method for calculations. The corresponding charts and block force diagrams are illustrated in **Figure 1**.

The stability factor calculation formula, as mentioned in reference [14], is as follows:

$$K=\frac{\sum_{i=1}^{n-1}\left(\left(\left(W_i\left(1-r_U\right)\cos\alpha_i-A\sin\alpha_i\right)\tan\varphi_i+C_iL_i\right)\prod_{j=i}^{n-1}\psi_j\right)+R_s}{\sum_{i=1}^{n-1}\left(\left(W_i\left(\sin\alpha_i+A\cos\alpha_i\right)+T_{D_i}\right)\prod_{j=i}^{n-1}\psi_j\right)+T_s} \tag{1}$$

In the formula:

$$R_n=\left(W_n\left(1-r_U\right)\cos\alpha_n-A\sin\alpha_n\right)-R_{D_n}\right)\tan\varphi_n+C_nL_n \tag{2}$$

$$T_n=\left(W_n\left(\sin\alpha_n+A\cos\alpha_n\right)+T_{D_n}\right. \tag{3}$$

$$\prod_{j=i}^{n-1}\psi_j=\psi_i\psi_{i+1}\psi_{i+2}KK\psi_{n-1} \tag{4}$$

In the formula:

Ψ_j is the transfer coefficient between adjacent blocks ($j=i$);

W represents the weight of the ith block (kN/m);

c represents the cohesion within the ith block (kPa);

φ represents the internal friction angle of the ith block (˚);

L represents the length of the sliding surface of the ith block (m);

α represents the inclination angle of the sliding surface of the ith block (˚);

β represents the water flow direction of the ith block (˚);

A represents the seismic acceleration;

r_U represents the pore pressure ratio;

K represents the stability coefficient.

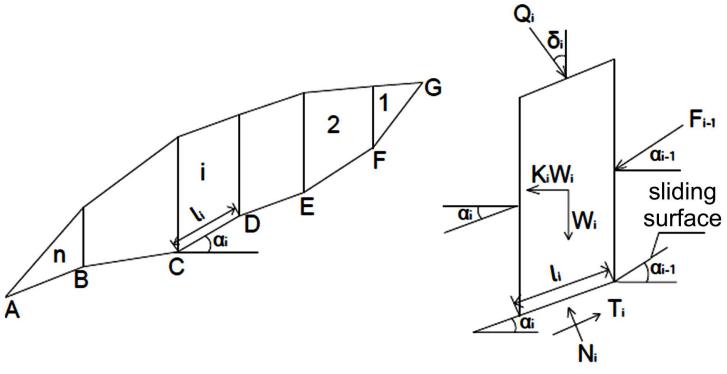

Figure 1. Slice graph and stress diagram of a slice.

2.2. Slope Stability Analysis with the Midas GTS NX 2019 Finite Element Method

Midas GTS NX 2019 is a geotechnical engineering software based on finite element strength analysis. It offers advanced window-based operations, powerful computational analysis capabilities, and modeling modules. It can handle various types of data processing and modeling using its built-in features, such as built-in modeling and grid generation. It allows for autonomous modeling by creating two-dimensional and three-dimensional solid models to simulate the changing state of soil and rock masses. The software presents the calculation results in the form of tables, images, animations, and more, providing an intuitive representation of stress-strain relationships within the soil. In particular, when simulating calculations for open slopes, mountain tunnels, and similar projects, the results closely resemble real-world conditions. The subject of this study is the slope at the Yuxi Riverside Bridge-Tunnel Connection of the Lujijiang Bridge, which features a unique geographical location and complex environmental conditions that make Midas finite element software an ideal choice.

Stability Factor Calculation Method:

The calculation in this study is based on Mohr-Coulomb theory and establishes a constitutive model. The entire analysis process involves nonlinear time history analysis combined with the strength reduction method (SRM). The definition of the stability factor in the strength reduction method is based on how much the internal shear strength of the slope decreases when the slope reaches a critical state. The calculation process is as follows: after the model is constructed, the stability factor of the slope is continuously reduced, and the corresponding calculation parameters are obtained. The reduced parameters, including the internal friction angle φ and cohesion c, are then input into the model formula for calculation. This process continues until the model experiences failure and reaches an unstable state. The value obtained just before failure is the stability factor K of the slope. The failure criterion is based on the Mohr-Coulomb yield criterion.

Model Formula [15]:

$$s = c'_{\min} + \left(\sigma_n - \mu\right)\tan\varphi' \tag{5}$$

The stability factor calculation formula [15] is as follows:

$$c_{\min} = c/K,\ \tan\varphi'_{\min} = \tan\varphi'/K \tag{6}$$

3. Comprehensive Analysis Method of Side Slope Stability

3.1. Analysis of Advantages and Disadvantages of the Limit Equilibrium Method

The limit equilibrium method has notable advantages. During calculations, it establishes a link between the stability factor and the potential sliding surfaces on the slope. It directly treats the sliding body as a rigid object, eliminating the need to consider its own deformation and effectively transforming many failure

problems into two-dimensional problems for resolution. Its structural model is simple to select, and it offers clear mechanical concepts during vector calculations, allowing for the rapid calculation of stability factors. In recent years, this method has gained wide recognition and been widely applied, leading to the development of various other methods, including the coefficient of transmission method used in this paper. Currently, the coefficient of transmission method, known for its simplicity, is most common in engineering applications [16].

However, this method does have some limitations. It requires certain conditions for the inferred sliding surfaces; specifically, the angles at discontinuities on the sliding surface should not be excessively large to avoid calculation errors. Furthermore, it does not consider the equilibrium between force and displacement. When a rigid body moves along a predefined failure surface, unrealistic force distributions can occur, particularly in cases of stress concentration. Additionally, this method primarily addresses two-dimensional problems. Complex three-dimensional analyses, which involve more unknown internal forces and vector calculations, may have limitations, such as convergence issues during calculations [17].

3.2. Analysis of Advantages and Disadvantages of the Midas GTS NX 2019 Finite Element Method

The use of finite element software for slope analysis has become increasingly common in engineering. The advantages of this method include not needing to predefine the position or shape of sliding surfaces; it can obtain information about the approximate sliding surface range, stress, and displacement of the slope through systematic calculations. Midas GTS NX 2019, as geotechnical analysis software, is highly regarded for its robust modeling capabilities and efficient data processing. Its support for strength reduction algorithms allows for the gradual reduction in internal parameters, leading to the slope's ultimate failure state and providing the desired results and various model representations. This method ensures a rigorous theoretical framework and can handle slopes with complex geometric shapes and boundary conditions, offering high calculation accuracy. It has significant potential for application in engineering projects [18] [19] [20] [21].

However, this method also has limitations. In the construction of finite element models, especially for complex slope environments, mesh generation can be challenging. The size of the model's boundary range significantly affects the accuracy of the calculation results, and sparse mesh division can lead to substantial errors. Therefore, precise control over the mesh density and boundary range is necessary. Additionally, when the slope undergoes significant deformation, convergence issues in the calculation results can arise.

3.3. Comprehensive Analysis of Slope Stability Using Limit Equilibrium and Finite Element Methods

As indicated above, both methods have unique characteristics, and the results

they yield may often differ. In practical applications, the multiple uncertainties associated with stability factors could impact subsequent analysis processes. Therefore, it is necessary to systematically analyze this issue and propose feasible solutions for more accurate slope assessments.

Hence, we propose using the analytic hierarchy process (AHP) to calculate the weights of the two methods in slope stability calculations separately. These calculated weights are then combined with the original stability factors through weighted summation to form a new formula for calculating the slope stability specific to the case. The specific steps are as follows.

Establish a hierarchical structure model based on the selected stability impact indicators, including the target layer, criterion layer, and scheme layer, as shown in Figure 2.

1) The structure model and the influence index are evaluated, and the comparative judgment matrix is constructed.

$A-C$ criterion layer contrast judgment matrix

$$B-A=\begin{pmatrix} 1 & 2 & 3 \\ 1/2 & 1 & 2 \\ 1/3 & 1/2 & 1 \end{pmatrix}$$

$B-C$ scheme layer contrast judgment matrix

$$C_1=\begin{pmatrix} 1 & 1/3 \\ 3 & 1 \end{pmatrix} \quad C_2=\begin{pmatrix} 1 & 2 \\ 1/2 & 1 \end{pmatrix} \quad C_3=\begin{pmatrix} 1 & 3 \\ 1/3 & 1 \end{pmatrix}$$

2) Calculate the vector for single-level ranking and conduct a consistency test. If the test is successful, the characteristic vector becomes the weight vector; if it fails, it is necessary to re-establish the comparison matrix.

Consistency test for the criteria level:

The maximum eigenvalue of the matrix λA = 3.0092; consistency index (CI) = (maximum eigenvalue − matrix order)/(matrix order − 1) = (3.0092 − 3)/(3 − 1) = 0.0046.

Referring to the index standard table, as shown in Table 1:

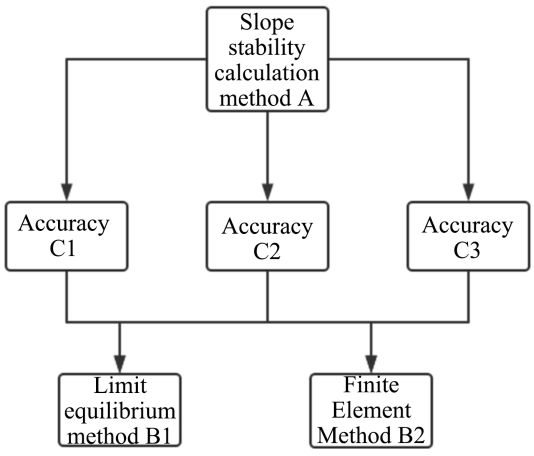

Figure 2. Hierarchy model diagram.

Table 1. Conformance indicator table.

Matrix order	n	1	2	3	4	5	6	7	8	9	10
	RI	0	0	0.58	0.90	1.12	1.26	1.32	1.41	1.45	1.49

With a consistency ratio (CR) of CR = 0.0046/0.58 = 0.0079, which is less than 0.1, the consistency test passes. Therefore, the characteristic vector for the criterion level is determined to be X1 = 0.5397, X2 = 0.2970, and X3 = 0.1634.

3) Scheme-layer consistency testing:

The eigenvalues are λC1 = 2, λC2 = 2, λC3 = 2; the consistency index (CI) is calculated as CI = (2 − 2)/(2 − 1) = 0, resulting in CR = 0, which is less than 0.1, passing the consistency test. Therefore, the characteristic vector for the scheme level is determined as follows:

For the first set of values: X4 = 0.25, X5 = 0.75. For the second set of values: X6 = 0.6667, X7 = 0.3333. For the third set of values: X8 = 0.75, X9 = 0.25.

4) Calculate the total ranking vector, which represents the relative importance of each indicator within a particular level to the overall hierarchy. Perform a test, and if it passes, these weight values can be used for decision analysis. The final weight values for each indicator are shown in **Table 2**.

Consistency Test: Calculating results in CI = 0, CR = 0/0.58 = 0, which is less than 0.1. Therefore, it passes the consistency test.

Through the calculations mentioned above, the AHP weights for the two methods in this computation are determined as follows: ω_{AHP} = (0.4555, 0.5445).

5) After obtaining the corresponding weight values, defining them as ω_1 and ω_2, the stability coefficients calculated by both methods, K_1 and K_2, are multiplied by ω_1 and ω_2, respectively, to obtain the new coefficients K_s. This constitutes the comprehensive analysis method, and the formula is as follows:

$$K_s = K_1\omega_1 + K_2\omega_2 \tag{7}$$

3.4. Slope Stability Evaluation

Based on the characteristics of the slope and its current state and with reference to relevant standards [22] [23], the stability factor evaluation criteria are divided as follows:

1) $K < 1.0$ Unstable;

2) $1.0 \le K < 1.05$ Slightly Unstable;

3) $1.05 \le K < 1.15$ Basically stable;

4) $K \ge 1.15$ Stable.

4. Engineering Case Analysis

4.1. Project Overview

The Yuchu Expressway Bridge is located at the junction of Yuxi City and Chuxiong Prefecture, and it is the first single-tower, single-span steel box girder cable-stayed bridge in China. The total length of the bridge is 798 m, spanning

Table 2. The final weight table of each index.

		Administrative levels (B)			Hierarchical combination weights (C)
		Accuracy	Usability	Simplicity	
Administrative levels (C)	Extreme equilibrium method	0.25	0.6667	0.75	0.4555
	Finite element method; finite element method	0.75	0.3333	0.25	0.5445

across the Lujijiang River. The bridge is surrounded by undulating and rugged mountainous terrain on both sides. The slope in question is situated on the right side of the Yuxi Riverside Tunnel and at the junction of the bridge piers, as shown in **Figure 3**. It is located between kilometers 102 + 300 and 102 + 600 on the Yuchu Expressway. The exposed soil layers in this slope area mainly consist of Quaternary residual slope deposits, underlain by Lower Cambrian deep gray thin- to thick-bedded dolomite and fractured shale.

Due to the constraints of the site's topography, excavation work is required for the construction of bridge piers, tunnels, and tunnel anchors. Given that most of the slopes in this area are steep rocky slopes and important structures such as bridges and tunnels are located beneath them, any failure could have serious consequences. According to the design plan, excavation will be carried out at the base of the slope to construct anchor foundations for the Yujichu Bridge tower cables. This change in slope conditions may lead to new deformations in the slope complex, potentially affecting construction safety. Moreover, it will be difficult to determine the stability status of the slope at that time. This area involves critical engineering structures such as the No. 0 bridge pier of the Lujijiang Grand Bridge, anchors for the Yuxi Riverside Tunnel, and the exit of the Dalishu Tunnel. To ensure construction safety, treatment of this slope is necessary.

4.2. Selection of the Calculation Parameters

Based on on-site survey data, indoor experiments, and the engineering geological analogy method, and in accordance with relevant standards such as the "Design Code for Landslide Prevention and Control in Highways" [24], relevant parameter values have been determined and are presented in **Table 3**, as shown below.

4.3. Selection of the Calculated Profile

In accordance with the relevant standards outlined in the "Design Code for Landslide Prevention and Control" [25] and based on field investigations, the typical cross-section labeled I-I was selected for calculations, as depicted in

Figure 3. Picture of slope position.

Table 3. Physical and mechanical parameters of the rock and soil mass.

Material name	Modulus of elasticity (GPa)	Serious (kN/m^3)	Saturation capacity (kN/m^3)	Cohesive strength c (kPa)	Internal frictional angle φ (˚)	Poisson's ratio
Strongly weathered, dolomitic limestone	0.043	26	26.5	62	22	0.3
Moderately weathered dolomitic limestone splinting test	2.0	26.5	27	178	57	0.28
Broken slate	0.013	25.5	26	102	39	0.3

Figure 4. The contour lines, scale, and other details shown in the figure are all based on on-site surveys.

4.4. Calculated by the Limit Balance Method

Following an on-site geological survey of the environmental conditions and in accordance with the relevant standards outlined in the "Design Code for Landslide Prevention and Control" [25], a typical cross-section labeled I-I was chosen for the stability calculations of the slope after excavation.

Based on the characteristics observed after excavating the slope and combining the investigation of surface deformations, fractures and cracks were observed at the front and rear edges of the slope. After conducting a physical exploration of the rock mass, it was determined that there is a transition zone between soft and hard rocks in the survey area, and the overall integrity of the rock mass at the transition zone is poor. Therefore, considering the supplementary survey, a potential sliding surface was identified by integrating all the information.

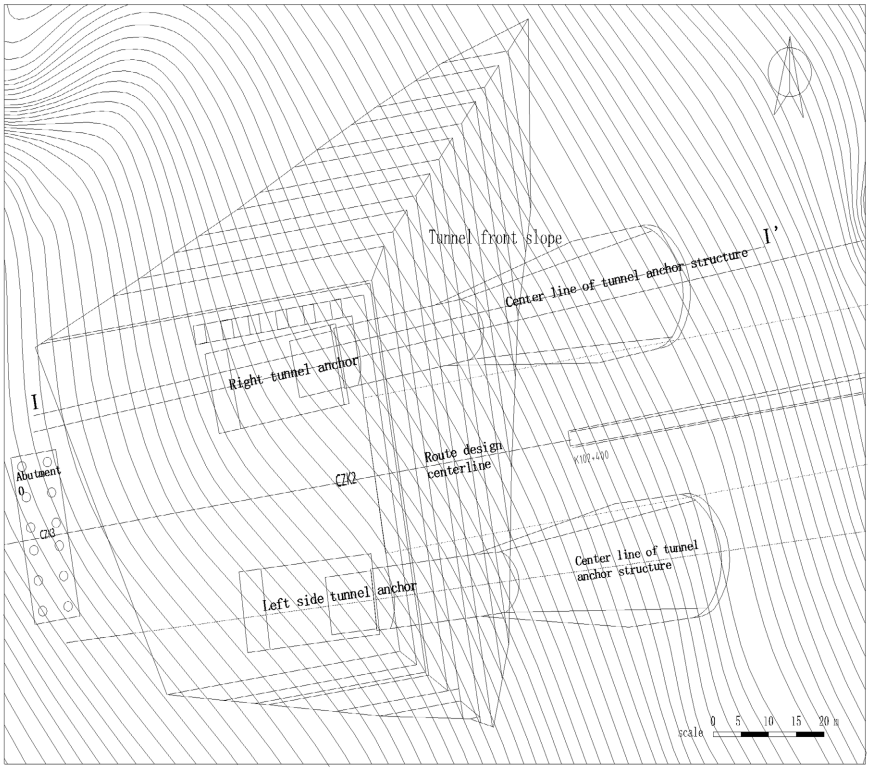

Figure 4. Plane layout of the Yuxi'an tunnel slope.

After dividing the selected cross-section of the slope, stability calculations were performed using Equation (1), resulting in the natural state cross-section of the slope, as shown in **Figure 5**.

Based on the calculations using the abovementioned method, the stability coefficient for the slope after excavation was found to be 1.06, indicating that it is in a stable state. The coefficient for the slope in the excavation state is also 1.06, indicating that it is in a condition of basic stability.

4.5. Midas GTS NX 2019 Finite Element Method Calculation

Based on an on-site topographic survey, it was determined that the front and rear edges of the slope had substantial separation with relatively mild terrain undulations. Considering the intricacies associated with the computational process, the decision was made to simplify the three-dimensional model into a two-dimensional representation. A cross-sectional profile that is deemed representative was selected for conducting finite element analysis, both for the slope's natural state prior to excavation and its postexcavation condition.

Utilizing survey data, a two-dimensional Mohr-Coulomb model was constructed employing Midas GTS NX 2019 software. The model's base possessed a length of 200 m, with a maximum elevation of 154 m and a minimum elevation of 89 m. The mesh division scheme for the slope's cross-sectional profile is illustrated in **Figure 6**.

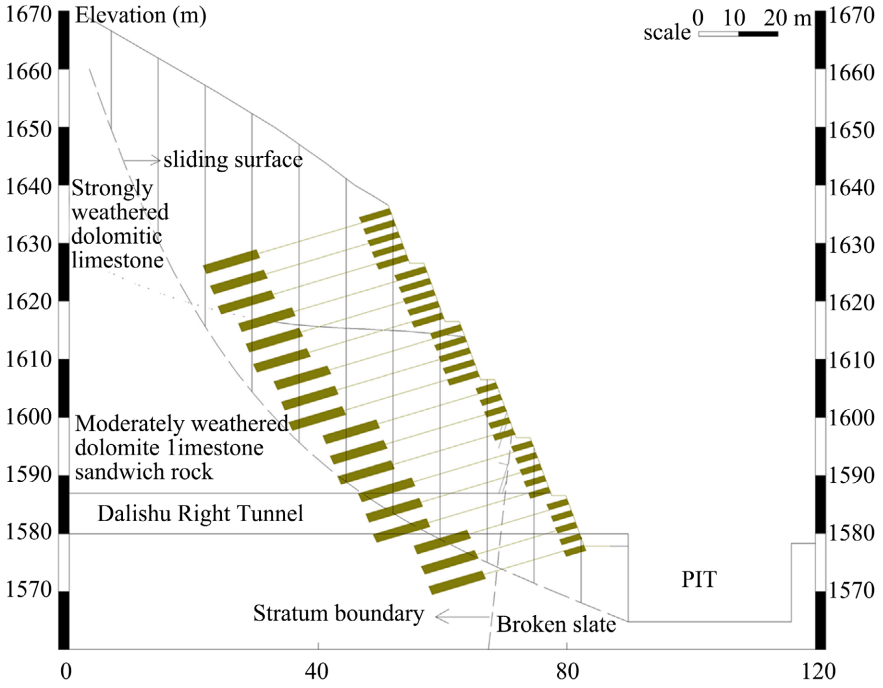

Figure 5. Sectional strip diagram of the unexcavated state.

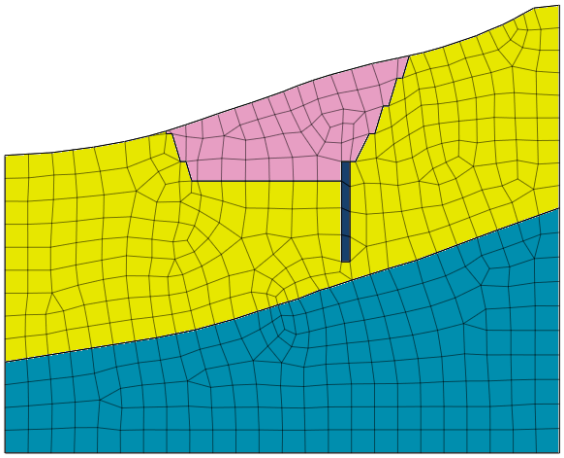

Figure 6. Grid division drawing of the section.

Following a comprehensive analysis using the SRM (Structural Response and Movement), displacement vector maps were computed and are presented in **Figure 7** and **Figure 8**. Stress distribution diagrams are depicted in **Figure 9** and **Figure 10**. Additionally, **Figure 11** and **Figure 12** illustrate the distribution of plastic zones before and after excavation.

1) Displacement vector maps display;

2) Stress distribution diagrams;

3) The plastic zone distribution diagrams.

Based on the calculations described above, the stability coefficients were obtained and are presented in **Table 4** as follows.

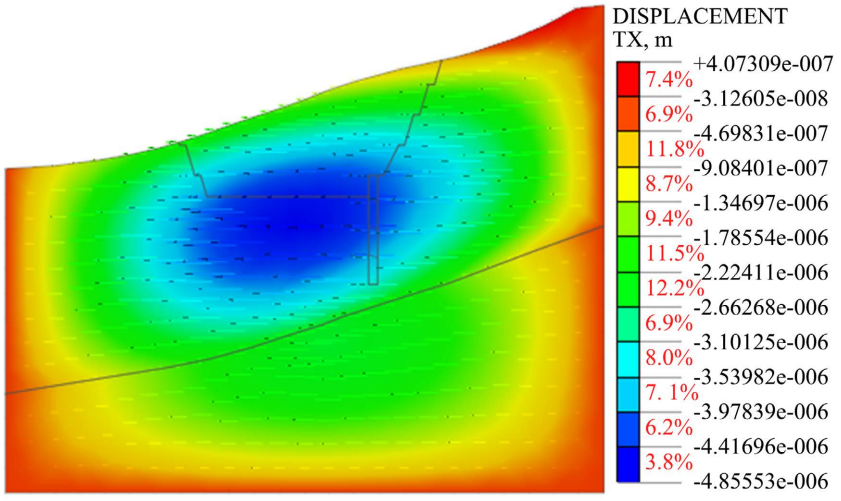

Figure 7. Unexcavated condition.

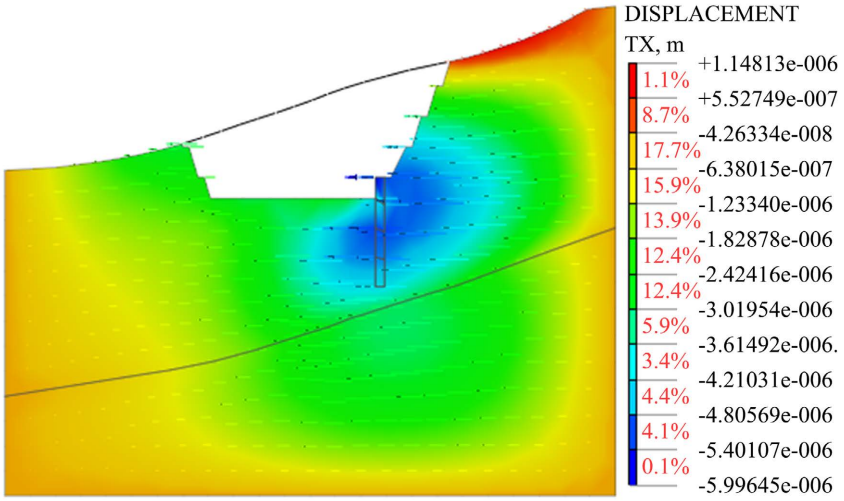

Figure 8. Excavated condition.

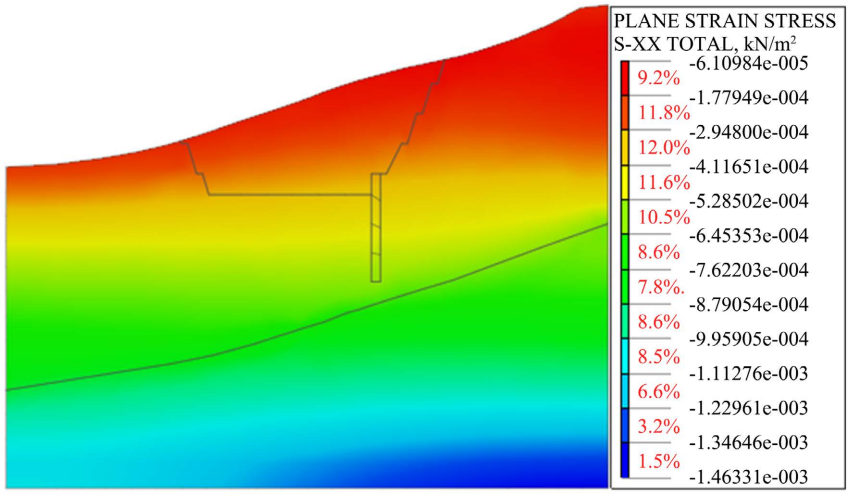

Figure 9. Unexcavated condition.

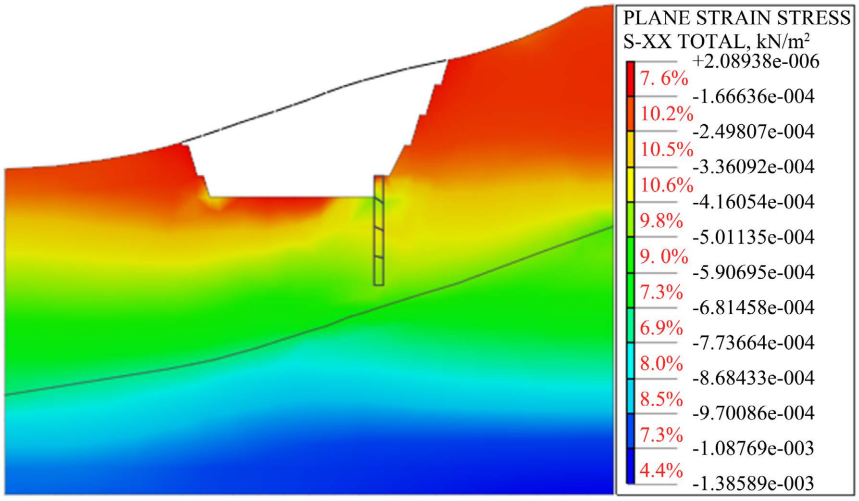

Figure 10. Excavated condition.

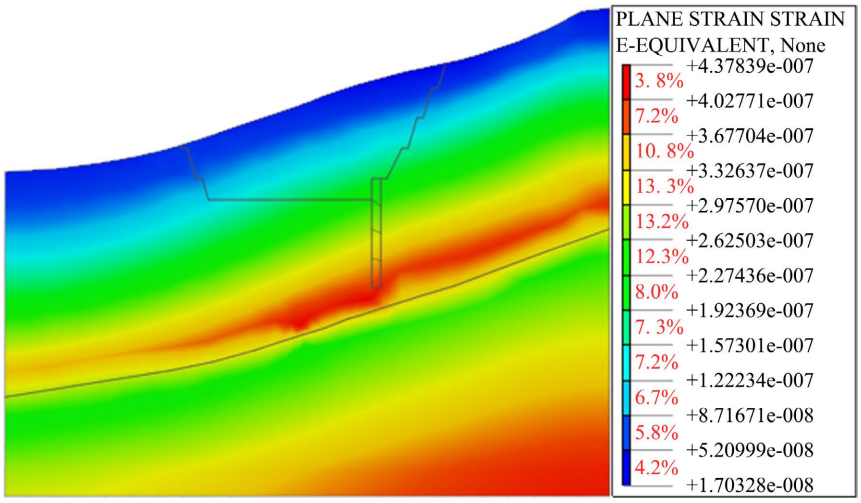

Figure 11. Unexcavated condition.

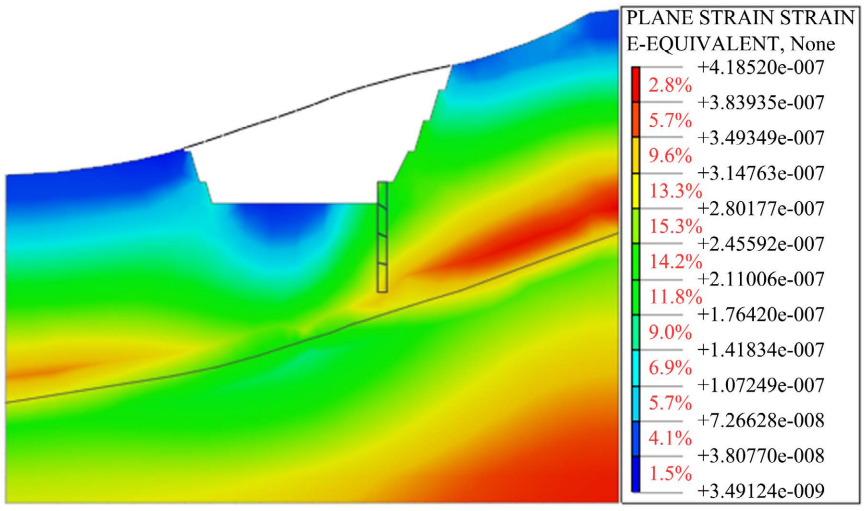

Figure 12. Excavated condition.

Table 4. Stability coefficient of Section I-I'.

Working condition	I-I'
Unexcavated condition	1.24
Excavated condition	1.12

Based on the calculation results, the coefficient for the natural, unexcavated state is 1.24, indicating stability. The coefficient for the excavated state is 1.12, indicating a state of basic stability.

4.6. Calculation of Comprehensive Analysis Method for Limit Equilibrium and Finite Element Slope Stability

Based on the results obtained from the two methods mentioned above, a comprehensive stability coefficient is calculated by combining the weights according to the formula. The results are presented in Table 5.

Based on the calculation results, under the comprehensive analysis method, in the natural, unexcavated state, the coefficient is 1.23, and the slope remains in a stable condition. In the excavated state, the coefficient is 1.09, indicating that the slope is in a state of basic stability. These results indicate compliance with the regulatory requirements. In both the natural unexcavated state and the excavated state, the slope maintains stability or basic stability in accordance with the specified standards.

5. Comparison of Stability Analysis Results

1) From the calculation results, it is apparent that the stability coefficients obtained through the limit equilibrium method are within the safe range but are smaller than those from the finite element method. The reason for this discrepancy lies in the fact that the segmentation method used in this case assumes a circular arc as the sliding surface of the slope, without accounting for the interaction forces between individual blocks. This leads to an underestimation of the results.

2) Midas GTS NX 2019, employing the SRM analysis method, was used to conduct calculations for slope stability, and the results fell within the safe range. Observing the displacement contour plots of the slope, a distinct blue displacement zone becomes evident after excavation, concentrated at the toe of the slope and the anti-slide pile area. Upon examining other contour plots, substantial alterations in the stress and plastic zone are observed at the toe and anti-slide pile area before and after slope excavation, yet the overall stability remains within the safe range. In contrast, the finite element method can effectively provide pertinent data concerning slope stability, with the sliding surface being computed based on actual data, resulting in more accurate and reliable analysis outcomes.

3) Through the example, it becomes apparent that the two methods exhibit numerical disparities under identical conditions. Hence, when utilizing these

Table 5. Comprehensive analysis stability coefficient of Section I-I'.

Working condition	I-I'
Unexcavated condition	1.23
Excavated condition	1.09

two methods for calculations, defining clear stability coefficients and offering an accurate and reliable evaluation proves challenging. To address this issue and improve calculation precision, the analytic hierarchy process (AHP) was utilized to determine the weights of stability-influencing factors for the two methods. Subsequently, the obtained weight values were combined with the stability coefficients of both methods, yielding a comprehensive slope stability analysis method based on both the limit equilibrium and finite element approaches.

4) Following calculations with the combined weights, the slope in both conditions maintains a state of basic stability and stability, in accordance with regulatory requirements. Consequently, the slope is assigned definitive stability coefficient values, providing analytical criteria for subsequent assessments and offering valuable guidance for optimizing slope stability calculations.

6. Conclusions

1) Both the limit equilibrium method and the Midas GTS NX 2019 finite element analysis method can accurately assess slope stability, and each possesses its own advantages and limitations. Notably, the limit equilibrium method tends to yield conservative results.

2) The limit equilibrium method provides clear mechanical concepts and results, making it suitable for slope stability analysis and theoretical research. However, its framework theory based on rigid body assumptions neglects the internal connections within the soil, yielding only approximate solutions. Additionally, the assumed sliding surface location reduces the calculation precision.

3) The finite element method considers the constitutive relationship of the soil, delineates the slope's sliding surface, and visually presents stress and strain variations within the soil through contour plots, offering a more distinct and intuitive effect. Nevertheless, challenges are encountered in determining model boundaries and meshing when conducting complex slope analyses.

4) Utilizing the analytic hierarchy process to ascertain the weights of stability-influencing factors for the two methods, an optimized calculation formula specific to the slope was proposed. It demonstrates feasibility and holds promise for application in expedited and effective stability assessments in future research, thereby enhancing work efficiency.

Conflicts of Interest

The authors declare no conflicts of interest regarding the publication of this paper.

References

[1] Jia, Z.B. (2020) Stability Analysis of Pre-Stressed Anchor Slope under Seismic Action. *Rock and Soil Mechanics*, **41**, 3604-3612.

[2] Li, S. (2020) Research on Instability Criterion of Slope Engineering Based on Mutation Characteristics. *Journal of Disaster Prevention and Mitigation Engineering*, **40**, 852-859.

[3] Yu, Y.X. (2020) Analysis on Deformation and Failure Mechanism and Control Scheme of High Rock Mass Slope on the West Side of Shunhang Temple in Xuelang Mountain. *Journal of Geological Hazards and Environment Preservation*, **31**, 33-43.

[4] Li, W.X. (2020) Qualitative and Quantitative Evaluation of Bank Slope Stability of Lixianjiang Bridge with Long Distance. *Geotechnical Mechanics*, **34**, 181-184.

[5] Zhao, S.J. (2012) Current Situation and Development of Slope Stability Analysis Methods. *Soil Engineering and Foundation*, **26**, 92-95.

[6] Geshu, K., Vipin, K., Sahil, S., *et al.* (2022) Geoenvironmental and Geotechnical Assessment of Soil Slopes in the Vicinity of Atal Tunnel in Himachal Pradesh, India. *Geomatics, Natural Hazards and Risk*, **13**, 1251-1269. https://doi.org/10.1080/19475705.2022.2068456

[7] Biao, Z. and Quanli, S. (2023) Upper Bound Analysis of the Anti-Seismic Stability of Slopes Considering the Effect of the Intermediate Principal Stress. *Frontiers in Earth Science*, **10**, Article ID: 1023883.

[8] Haziq, I.R., Aizat, T.M., Norinah, R.A., *et al.* (2023) Slope Stability Analysis of Riverbank in Malaysia with the Effects of Vegetation. *Physics and Chemistry of the Earth*, **129**, Article ID: 103334. https://doi.org/10.1016/j.pce.2022.103334

[9] Li, C.C. and Håvard, A.H. (2023) An Issue in the Current Definition of the Factor of Safety for Rock Slopes and Suggestions for Improvement. *IOP Conference Series: Earth and Environmental Science*, **1124**, Article ID: 012105. https://doi.org/10.1088/1755-1315/1124/1/012105

[10] Wu, J.Q. (2018) The Role of Manifold Method in Stability Analysis of Open-Pit to Underground Mining Slope. *Mining Research and Development*, **38**, 62-66.

[11] Chen, Z.Y. (2001) Discussion on "Three-Dimensional Limit Equilibrium Analysis Method and Its Application in Slope Stability". *Chinese Journal of Geotechnical Engineering*, **23**, 127-128.

[12] Zhou, X., Fu, D., Wan, J., *et al.* (2023) The Shear Strength of Root-Soil Composites in Different Growth Periods and Their Effects on Slope Stability. *Applied Sciences*, **13**, 11116. https://doi.org/10.3390/app131911116

[13] Yang, X., Shuang, L., Huanran, W., *et al.* (2023) Strengths and Infinite Slope Stability of Unsaturated Soils. *International Journal of Geomechanics*, **23**. https://doi.org/10.1061/IJGNAI.GMENG-9021

[14] Zhou, L. (2010) Application of Limit Equilibrium Method and FLAC3D in Landslide Stability Analysis. *China Water Transport*, **10**, 194-196.

[15] Zhang, D. (2019) Application of MIDAS-GTS in Landslide Stability Analysis and Engineering Treatment. *World Nonferrous Metals*, No. 14, 229-231.

[16] Zhang, R.H. (2021) Stability Analysis of Multi-Stage Homogeneous Loess Slope Based on Improved Limit Equilibrium Method. *Rock and Soil Mechanics*, **42**, 813-825.

[17] Villalobos Felipe, A. (2020) Effect of Nail Spacing on the Global Stability of Soil Nailed Walls Using Limit Equilibrium and Finite Element Methods. *Transportation*

Geotechnics, **2020**, Article ID: 100454. https://doi.org/10.1016/j.trgeo.2020.100454

[18] Jin, Y.C. (2021) Slope Stability Analysis Based on the Limit Equilibrium Method and Strength Reduction Method. *Transportation Geotechnics*, **631**, Article ID: 012048. https://doi.org/10.1088/1755-1315/631/1/012048

[19] Zoning, S., Tao, L. and Shuo, M. (2019) Soil Parameters Inversion and Influence Based on MIDAS GTS. *IOP Conference Series*: *Earth and Environmental Science*, **384**, Article ID: 012126. https://doi.org/10.1088/1755-1315/384/1/012126

[20] Szilvágyi, Z. and Ray, R.P. (2018) Verification of the Ramberg-Osgood Material Model in Midas GTS NX with the Modeling of Torsional Simple Shear Tests. *Periodica Polytechnica Civil Engineering*, **62**, 629-635.

[21] Tao, X. (2015) The Application and Analysis of Midas/GTS in Landslide Control. *International Journal of Engineering Research*, **4**, 409-411. https://doi.org/10.17950/ijer/v4s8/802

[22] GB 50585-2010 (2010) Code for Investigation of Geotechnical Engineering. National Standards of the People's Republic of China, Beijing.

[23] JTG C20-2011 (2011) Specification for Geotechnical Investigation of Highway Engineering. Industry Standard-Transportation, Beijing.

[24] JTG-T 3334-2018 (2018) Design Specification for Landslide Prevention and Control of Highways. Industry Standard-Transportation, Beijing.

[25] GB/T 38509-2020 (2020) Design Specification for Landslide Prevention and Control. State Administration for Market Regulation, Beijing.